THE JOURNAL OF PHYSICAL CHEMISTRY B

ARTICLE

pubs.acs.org/JPCB

Molecular Dynamics in Rod-Like Liquid Crystals Probed by Muon Spin Resonance Spectroscopy

Iain McKenzie,[*,†,§] Robert Scheuermann,[‡] Kamil Sedlak,[‡] and Alexey Stoykov[‡]

[†]ISIS Facility, Rutherford Appleton Laboratory, Didcot, Oxon, United Kingdom

[‡]Laboratory for Muon Spin Spectroscopy, Paul Scherrer Institute, Villigen AG, Switzerland

Supporting Information

ABSTRACT: Muoniated spin probes were produced by the addition of muonium (Mu) to two rod-like liquid crystals: *N*-(4-methoxybenzylidene)-4′-*n*-butylaniline (MBBA) and cholesteryl nonanoate (CN). Avoided level crossing muon spin resonance spectroscopy was used to characterize the muoniated spin probes and to probe dynamics at the molecular level. In MBBA Mu adds predominantly to the carbon of the bridging imine group and the muon and methylene proton hyperfine coupling constants (hfccs) of the resulting radical shift in the nematic phase due to the dipolar hyperfine coupling, the ordering of the molecules along the applied magnetic field and fluctuations about the local director. The amplitude of these fluctuations in in the nematic phase of MBBA is determined from the temperature dependence of the methylene proton hfcc. Mu adds to the double bond of the steroidal ring system of CN and the temperature dependence of the Δ_1 line width provides information about the amplitude of the fluctuations about the local director in the chiral nematic phase and the slow isotropic reorientation in the isotropic phase.

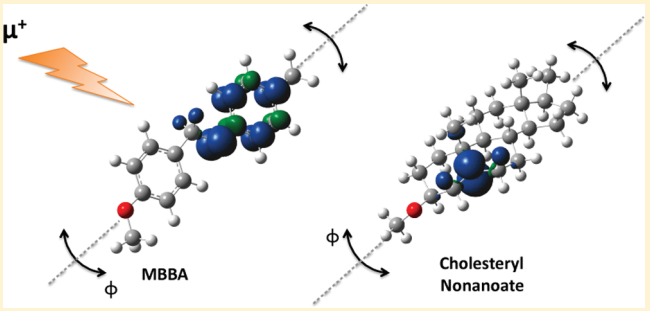

INTRODUCTION

Liquid crystals (LC) are materials that form phases with a degree of order between the disorder of the liquid or isotropic (I) phase and the regular structure of crystalline (Cr) phases.[1−3] The molecules that make up a LC have anisotropic shapes, such as rods (calamitic LC) or disks (discotic LC). Rod-like molecules can form a wide range of mesophases but the most common is the nematic phase (N), where the molecules' positions are disordered but the long molecular axes on average point along a preferred direction known as the director ($\hat{n}$). The order in a LC is quantified using the order parameter, *S*, which is defined by

$$S = \int \frac{1}{2}(3\cos^2\theta - 1) f(\theta)\, d\Omega \qquad (1)$$

where θ is the angle between the rotation axis of a rod-like molecule and the director and $f(\theta)\, d\Omega$ is the fraction of molecules in a solid angle $d\Omega$ that are oriented at an angle θ.[1]

N-(4-Methoxybenzylidene)-4′-*n*-butylaniline (MBBA) is a rod-like LC containing two phenyl rings with an imine linkage (Figure 1). MBBA was the first material to be produced that forms a N phase around room temperature and it has been extensively studied by a wide range of experimental techniques. There is a I to N phase transition at $T_{N-I} \approx 314-320$ K and a N to Cr phase transition at ∼290−295 K, with the phase transition temperatures depending on the heating and cooling rates. The order parameter of MBBA has been measured as a function of temperature, and Kneppe et al. have shown that it can be approximated by

$$S = \left(1 - \frac{T}{T^*}\right)^{0.188} \qquad (2)$$

where $T^* \approx T_{N-I} + 1$.[4]

Rod-like molecules with chiral centers can form the chiral nematic (or cholesteric) phase (N*), where there is orientational ordering of the molecules along $\hat{n}$ as in the N phase, but with $\hat{n}$ rotating gradually throughout the sample, generating a helical director configuration with the axis of this rotation normal to $\hat{n}$. Cholesteryl nonanoate (CN) is a rod-like LC that is a derivative of cholesterol and possesses 8 chiral centers (Figure 2). Cooling CN results in a I to N* phase transition at 364.3 K and a N* to Smectic A (SmA) phase transition at 348.2 K.[5]

Many of the techniques for analyzing LC, such as polarizing optical microscopy or differential scanning calorimetry, do not provide any insight into the motion of the constituent molecules. It is important to study the molecular dynamics in LC and to determine how this relates to the bulk properties. Magnetic resonance techniques can provide information about the dynamics and ordering of the LC molecules. NMR has been used extensively to study LC but the difficulty in analyzing systems

Received: March 31, 2011
Revised: June 24, 2011
Published: July 12, 2011

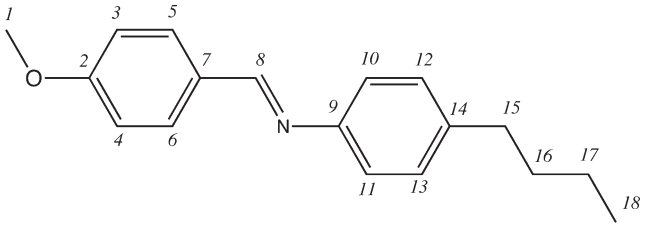

Figure 1. Structure of the liquid crystal *N*-(4-methoxybenzylidene)-4′-*n*-butylaniline (MBBA) and the numbering scheme for carbon atoms used in this paper.

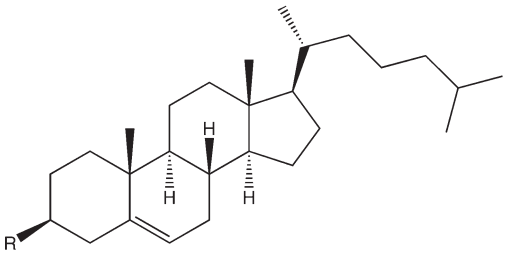

Figure 2. Structure of cholesteryl nonanoate (CN). R = O—C(═O)—C_8H_{17}.

with large numbers of ^{1}H in anisotropic environments has meant that it is often restricted to studying small solute molecules or partially deuterated LC molecules.[6,7] Pines and Chang studied MBBA using proton-decoupled ^{13}C NMR spectroscopy and found that the line positions shift in the N phase due to the preferential alignment of the molecules' long axis along the applied magnetic field and that the angle between the rotation axis and the O−CH3 bond is approximately 54.7°.[8] Dong and Shen probed the dynamics of the butyl chain and rotational diffusion by measuring quadrupolar splittings and spin relaxation rates of partially deuterated MBBA and they determined the activation energy for rotational diffusion about the long molecular axis to be 43.4−45.0 kJ mol^{-1} and perpendicular to the long axis to be 47.8−50.0 kJ mol^{-1}, depending on the high-frequency cutoff used in their fits.[9] Electron paramagnetic resonance (EPR) has been used to study several stable paramagnetic spin probes dissolved in MBBA.[10−13] The paramagnetic spin probes are very sensitive and highly selective so there generally are not a multitude of overlapping features in the spectra, however the structures of the spin probes are very different from the LC in which they are dissolved, so it can be argued that the measurements do not reflect the natural state of the LC.

There have been fewer magnetic resonance studies of CN. Luz et al. studied selectively deuterated CN and deuterated probe molecules in CN with ^{2}H NMR.[14] The order parameter was determined from the ^{2}H quadrupolar splitting and they also measured translational diffusion coefficients. In the N* phase there was a mixture of domains with the helical axes aligned along the field and domains with random orientation. We are not aware of any studies of paramagnetic spin probes in CN.

Ideally one would want to study paramagnetic spin probes whose structure is almost identical to that of the LC. Such spin probes can be produced by the addition of muonium (Mu), a light isotope of hydrogen with a positive muon as the nucleus, to unsaturated bonds in the LC.[15] Positive muons are radioactive particles with a spin of 1/2, a lifetime of 2.2 μs, a magnetic moment 3.183 times that of the proton and a mass approximately one-ninth that of the proton. In these muoniated radicals the unpaired electron interacts with the muon and with any nuclei in the radical with nonzero spin and the strength of the interaction between the unpaired electron and the nucleus "X" is the hyperfine coupling constant (hfcc), A_X. The structure, configuration and confirmation of a radical can be determined by measuring the magnitude and temperature dependence of the hfccs.[16] The hfccs are the sum of an isotropic component due to the Fermi contact interaction (A_X^{iso}) and an anisotropic component due to dipolar coupling between the electron and nuclear spins (denoted D_X if the hyperfine tensor has axial symmetry).

A series of experimental techniques collectively known as muon spin rotation/resonance/relaxation or μSR are used to probe the structure and dynamics of free radicals in soft matter, solids, liquids and gases.[17−20] These techniques involve injecting a beam of spin-polarized positive muons into a sample and detecting the positron produced by the decay of each muon. High-intensity muon beams are available at several facilities (Paul Scherrer Institute, Switzerland; ISIS, U.K.; TRIUMF, Canada; J-PARC, Japan) with a muon spin polarization of approximately 100%. The decay of the muon results in a positron being emitted preferentially along the direction of the muon's spin, which provides a convenient way to monitor the evolution of the muon spin and the muon's lifetime (2.2 μs) is convenient as it is comparable to many molecular processes. μSR has many features in common with EPR but has some advantages over it in studying spin probes in LC, such as the spin labeling occurs in situ and the muon being a much smaller perturbation than the stable free radicals currently used in EPR.

The avoided level crossing muon spin resonance (ALC-μSR) spectroscopic technique is used extensively to study the structure and dynamics of free radicals. The ALC-μSR technique involves measuring the asymmetry of the muon decay as a function of a magnetic field applied parallel to the initial direction of the muon spin. The asymmetry parameter is defined as $(n\mathrm{B} - n\mathrm{F})/(n\mathrm{B} + n\mathrm{F})$, where nF is the total number of positrons detected in the forward counters and nB is the total number of positrons detected in the backward counters, and is proportional to the muon polarization, P_z. In high magnetic fields the eigenstates of the radical can be approximated by pure Zeeman states, so there is no evolution of the muon's spin with time and the asymmetry is independent of the magnetic field. At specific values of the applied magnetic field nearly degenerate pairs of spin states can be mixed through the isotropic and anisotropic components of the hyperfine interaction. The muon polarization oscillates between the two mixing states and this leads to a loss of time-integrated asymmetry. There are three types of resonances, which are characterized by the selection rule $\Delta M = 0, \pm 1$ and ± 2, where M is the sum of the m_z quantum numbers of the muon, electron and proton spins. The resonances are referred to as Δ_0, Δ_1 and Δ_2 resonances, respectively. The Δ_2 resonance is extremely weak and is rarely observed.

The Δ_1 resonance field is given by

$$B_{\mathrm{res}}^{\Delta_1} = \frac{A_\mu}{2\gamma_\mu} - \frac{A_\mu}{2\gamma_e} \qquad (3)$$

where A_μ is the muon hfcc, γ_μ is the muon gyromagnetic ratio, and γ_e is the electron gyromagnetic ratio.[15] The Δ_1 resonance arises from mixing between spin states with the same electron and proton spins but different muon spin directions. These spin

states are mixed only in the presence of anisotropy, so the Δ_1 resonance can be considered to be diagnostic of a frozen state, anisotropic motion or slow isotropic reorientation. The shape of the resonance is sensitive to the motion of the radical and has a characteristic shape depending on the sign and magnitude of D_μ.

The Δ_0 resonance is due to mixing between spin states that have the same electron spin but opposite muon and proton spins and is observed for muoniated radicals in the solid, liquid or gas phases. The Δ_0 resonance field depends on both the muon hfcc and the proton hfcc, A_p, and is given by

$$B_{res}^{\Delta_0} = \frac{1}{2}\left[\frac{A_\mu - A_p}{\gamma_\mu - \gamma_p} - \frac{A_\mu + A_p}{\gamma_e}\right] \quad (4)$$

where γ_p is the proton gyromagnetic ratio.[15]

ALC-μSR has been used to study the local environment and dynamics of muoniated spin probes in a variety of soft matter systems.[21−25] Lovett et al.[26,27] and McKenzie et al.[28] have studied the structure and dynamics of the cyclohexadienyl-type radicals produced by the addition of Mu to the calamitic LC 4-*n*-pentyl-4′-cyanobiphenyl (5CB). McKenzie et al. have also studied muoniated spin probes in the rod-like LC 4-*n*-octyl-4′-cyanobiphenyl (8CB)[29] and the discotic LC 2,3,6,7,10,11-hexahexyloxytriphenylene (HAT6).[30] In 5CB and 8CB the methylene proton hfccs shift due to the dipolar hyperfine coupling, the ordering of the molecules along the applied magnetic field and the fluctuations of the molecules about the director. In HAT6 an unusually broad and intense resonance was observed due to rapid electron spin relaxation that results from the intermittent overlap of the radical's π-system with those of neighboring HAT6 molecules.

In this paper we employ ALC-μSR spectroscopy to characterize muoniated spin probes in the two rod-like LC, MBBA and CN, and demonstrate that the muoniated spin probes provide information about the dynamics of these LC at the molecular level. We are concerned with probing director fluctuations, which involve collective motions of a large number of molecules and can provide information on molecular properties such as elastic constants and viscosities.

EXPERIMENTAL SECTION

MBBA and CN were purchased from Sigma Aldrich and were used without further purification. Oxygen was removed by melting the samples in a nitrogen atmosphere and bubbling with nitrogen gas for approximately two hours. It is necessary to remove O_2 from the samples because the Heisenberg spin-exchange reaction can broaden the resonances in the ALC-μSR spectra.[31] The degassed samples were sealed in aluminum cells with an internal volume of 3 mL and 20 μm titanium foil windows. The ALC-μSR experiments were performed using the ALC spectrometer at the πE3 beamline of the Paul Scherrer Institute in Villigen, Switzerland.[32] The experimental setup and technique have been described in detail in previous publications.[15,18]

The samples were melted and the ALC-μSR spectra were obtained at several temperatures as the sample was slowly cooled. The samples were left for 15−30 min to equilibrate at a given temperature before measurements were made and several field scans were obtained at each temperature (each taking at least 45 min) in order to obtain a sufficient signal-to-noise ratio. No changes were observed in the ALC-μSR spectra as a function of time at a given temperature, so we conclude that the sample was at thermal equilibrium when the measurements were made. All of the ALC-μSR spectra of MBBA were measured between 1.20 and 1.55 T with a step size of 1 mT, except at 310 and 315 K where ALC-μSR spectra were also obtained from 1.10 to 2.20 T with a step size of 1 mT. The magnetic field was always greater than 1.1 T in order to produce an oriented monodomain with the $\hat{n}$ aligned along the magnetic field. The ALC-μSR spectra of CN in the I and N* phases were measured between 1.35 and 1.90 T with a step size of 2 mT. These magnetic fields are insufficient to align the CN sample as Luz et al. noted that a field of 6 T was required to align the helical axis along the magnetic field, thus the sample consists of many small domains with randomly oriented helical axes and the spectra can be analyzed assuming a powder pattern.[14]

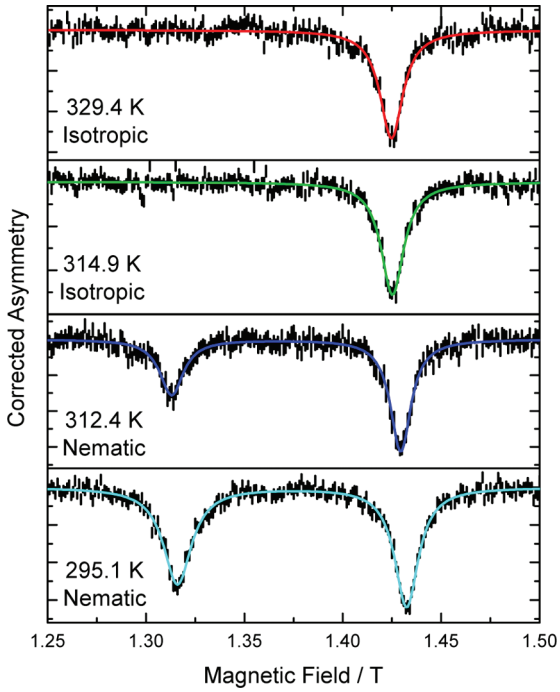

Figure 3. ALC-μSR spectra of Mu adduct of MBBA in the isotropic and nematic phases.

ALC-μSR spectra have a large field-dependent background that is very sensitive to the stopping position of the muons. It was not possible to remove the background by subtracting the spectrum of a substance that does not have resonances in the ALC-μSR spectrum (such as water) as we have found that the background is very sensitive to the density of the sample. Each resonance was fit with a single Lorentzian function and a fifth order polynomial was used to model the background. The fitting was performed with the MINUIT function minimization library in the ROOT package from CERN.[33]

All ab initio calculations were performed using the Gaussian 03 package.[34] In order to save computational resources the butyl chain of MBBA was replaced with a methyl group, the alkyl ester chain of CN was replaced by a methoxy group and the alkyl group at carbon 17 of CN was replaced by a methyl group. The geometries of the Mu adducts of MBBA were optimized with the unrestricted B3LYP density functional and the 6-311G(d,p) basis set while those of the Mu adducts of CN were optimized using the same density functional but the 6-31G(d,p) basis set. The hfccs for all radicals were calculated using the unrestricted PBE0 functional and the EPR-II basis set. These theoretical

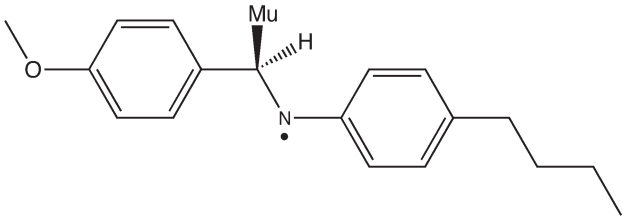

Figure 4. Structure of the radical formed by Mu addition to the bridging carbon of MBBA (Mu-C_8-MBBA).

methods have been demonstrated to give hfccs close to the experimental values.[35] Mu is almost chemically identical to H but its lower mass means that the vibrationally averaged C−Mu bond is approximately 4.9% longer than the corresponding C−H bond and the methylene C−H bond is reduced by approximately 0.3%.[17] Empirical correction factors of 1.20 and 0.94 were applied to the muon and methylene proton hfccs, respectively, in order to account for the effect of the light mass of the muon.[36] The muon hfccs were calculated by including a factor of 3.183 to account for the larger gyromagnetic ratio of the muon.

RESULTS AND DISCUSSION

MBBA. ALC-μSR spectra of MBBA were obtained at several temperatures in the I and N phases (Figure 3). There are two strong resonances in the ALC-μSR spectra of the N phase at ∼1.31 and 1.43 T and two weaker resonances at 1.70 and 1.97 T, with all but the lowest field resonance also being present in the I phase, suggesting that it is a Δ_1 resonance. The disappearance of the resonance at ∼1.31 T is reversible and is assumed to correspond to $T_{N-I} \approx 314$ K. The presence of a Δ_1 resonance in the N phase indicates that there is significant dipolar coupling, which is unlike the Mu adducts of the cyanobiphenyl LC.

The first steps in the analysis of the ALC-μSR spectra are to identify the resonances and assign them to specific radicals, which is done by comparing the experimental hfccs with values obtained from the DFT calculations and the results of previous studies on muoniated free radicals. Multiple radicals can form by Mu addition to MBBA and these can be divided into three classes: (1) substituted cyclohexadienyl radicals formed by Mu addition to the two phenyl rings, (2) the N-adduct of the imine group, and (3) the C-adduct of the imine group. Empirical evidence suggests that the two strong resonances are not due to either substituted cyclohexadienyl radicals or the Mu adduct of the N atom of the bridging imine group. Large numbers of substituted cyclohexadienyl radicals have been studied and the hfccs are too large to have resonances in the appropriate field range. For example, four types of cyclohexadienyl radical were formed by Mu addition to 5CB with A_μ between 446 and 491 MHz, which results in 1.64 $T < B^{\Delta}_{res1} < 1.80$ T and 1.81 $T < B^{\Delta}_{res0} < 1.99$ T. Addition at the nitrogen atom can be ruled out as the muon hfcc of the resulting radical would be by very small and negative since the N-Mu bond lies in the nodal plane of the π-system, analogous to the Mu adduct of the nitrogen atom of pyridine.[37]

The radical that most likely produced the observed resonances is the Mu adduct of the bridging carbon (structure shown in Figure 4 and henceforth referred to as the Mu-C_8-MBBA radical). DFT calculations were performed on this radical in order to confirm the assignment. The fully optimized structure has the two phenyl rings coplanar with the $C_7-C_8-N-C_9$ plane. A_μ and A_p are very sensitive to the orientation of the phenyl rings, which should be very mobile in the N and I phases, so the structure was also partially optimized with the phenyl rings perpendicular to the $C_7-C_8-N-C_9$ plane as in this configuration the π-systems of the phenyl rings will not overlap with the p-orbital of nitrogen and mimics the phenyl rings freely rotating. These two calculations (Table 1) give upper and lower limits for the muon and methylene proton hfccs and resonance fields. The experimental resonance fields fall within the range obtained from the DFT calculations, which confirms the assignment.

The averaged muon hfccs in the N phase, $\langle A_\mu \rangle$, were calculated from $B^{\Delta_1}_{res}$ using eq 3. $\langle A_\mu \rangle$ was not used to calculate $\langle A_p \rangle$ since it includes a dipolar contribution. Instead we note that it has been demonstrated for radicals containing a methylene (CHMu)

Table 1. Calculated Muon and Methylene Proton Hyperfine Coupling Constants (MHz) for the Mu Adduct of the Bridging Carbon of MBBA (UB3LYP/6-311G(d,p)//UPBE0/EPR-II) and the Corresponding Resonance Fields (T) with the Two Phenyl Rings Either Co-Planar or Perpendicular to the $C_7-C_8-N-C_9$ Plane

orientation	A_μ [a]	$B^{\Delta_1}_{res}$	A_p [b]	$B^{\Delta_0}_{res}$
coplanar	296.96	1.0902	73.08	1.1975
perpendicular	460.61	1.6910	113.36	1.8575

[a] A_μ calculated by multiplying DFT value by 3.183 to account for γ_μ/γ_p and by 1.20 to account for the primary isotope effect. [b] A_p calculated by multiplying DFT value by 0.94 to account for the secondary isotope effect.

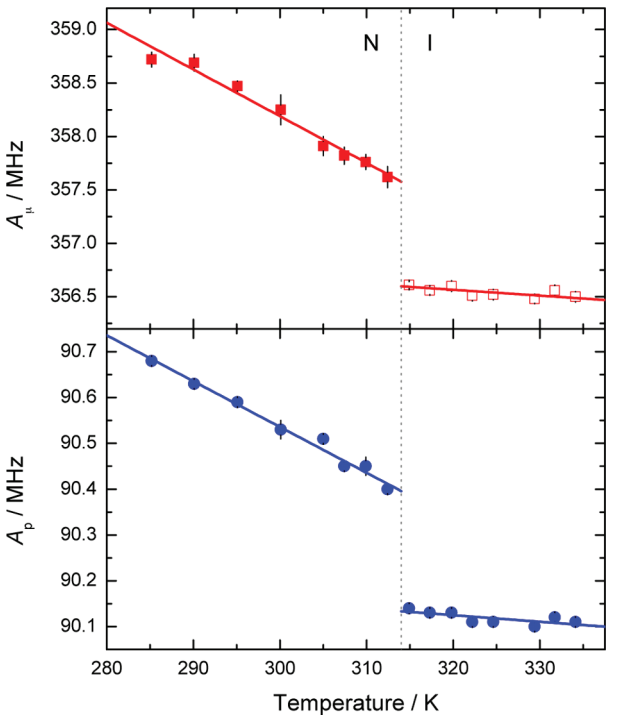

Figure 5. Muon and proton hyperfine coupling constants of the radical formed by Mu addition to the bridging carbon of MBBA (Mu-C_8-MBBA) as a function of temperature in the isotropic and nematic phases. The open squares denote muon hfccs obtained assuming $A_\mu/A_p = 3.956$. The dotted vertical line denotes the approximate position of the nematic−isotropic phase transition.

dx.doi.org/10.1021/jp203006w |J. Phys. Chem. B 2011, 115, 9360–9368

Table 2. Resonance Fields (T) and Muon Hyperfine Coupling Constants (MHz) of Mu Adducts of MBBA As a Function of Temperature

temp./K	$B_{res}^{\Delta_0}$	A_μ[a]	$B_{res}^{\Delta_0}$	A_μ[a]
309.9	1.7028(6)	415.7(1)	1.9691(9)	480.7(2)
314.9	1.6984(6)	414.6(1)	1.9669(6)	480.2(1)

[a] Hfccs calculated assuming $A_\mu/A_p = 4.123$.

group that both the isotropic and dipolar muon and methylene proton hfccs are proportional to each other.

$$A_\mu = KA_p \tag{5}$$

The main contribution to K is the γ_μ/γ_p ratio, which has a value of 3.183, and the rest results from the mass dependence of the molecule's vibrational modes. K was chosen to be 3.956 as this value produces $B_{res}^{\Delta_1}$ consistent with experiment, so we can calculate A_p, and hence A_μ, solely from $B_{res}^{\Delta_0}$ using eq 4 and eq 5. The values of A_μ and A_p as a function of temperature are shown in Figure 5 and a comparison with the DFT calculated values suggests that the phenyl rings are mobile but not freely rotating. Hoshino et al. found that the twist angles in MBBA are 33° for the N-side phenyl ring and 20° for the C-side phenyl ring.[38]

The resonances at ~1.70 and 1.97 T are assumed to be Δ_0 since they are present in both the N and I phases. The amplitude of the resonances indicates that they are not due to nuclei with small hfccs in the Mu-C_8-MBBA radical but are methylene proton resonances of other types of radicals. No Δ_1 resonances were observed, which suggests that the dipolar hfccs in these radicals is small. These radicals are assumed to be substituted cyclohexadienyl radicals that formed by Mu addition to the phenyl rings of MBBA as the resonance fields fall within the range typical for cyclohexadienyl radicals. The muon hfccs (Table 2) were calculated assuming that $A_\mu/A_p = 4.123$, the value determined for the C_6H_6Mu.[39] These muoniated cyclohexadienyl radicals will not be considered further as the lack of significant dipolar coupling means that they not suitable probes of ordering and dynamics in the N phase.

The muon and methylene proton hfcs of Mu-C_8-MBBA in the I phase are almost independent of temperature. The temperature dependence of A_μ and A_p are so low because the increased rotational motion about the N−C_9 bond, which increases the spin density on the nitrogen atom, counteracts the decrease in the hfcs due to vibrational motion of the CHMu group. There is a large increase in the hfccs at T_{NI} and they increase linearly as the temperature was lowered. The isotropic proton hfcc in the N phase (A_p^{iso}) was extrapolated from the hfccs in the I phase. This accounts for the changes in the hfccs that result from intramolecular effects.

The Mu-C_8-MBBA radical has axially symmetric muon and methylene proton hyperfine tensors due to rapid rotation around the "long" molecular axis; one component ($D_X^{\parallel}$) is parallel to the axis of rotation and two components are perpendicular ($D_X^{\perp}$). The dipolar tensor is by definition traceless so

$$D_X^{\parallel} = -2D_X^{\perp} \tag{6}$$

Table 3. Temperature Dependence of the Proton Dipolar hfcc of Mu-C_8-MBBA and Maximum Fluctuation Angle, ϕ_c, in the N Phase of MBBA

T/K	$\langle D_p^{\parallel}\rangle$/MHz	ϕ_c/radians
285.2	0.80 ± 0.02	0.194 ± 0.052
290.1	0.77 ± 0.02	0.122 ± 0.068
295.1	0.73 ± 0.01	0.267 ± 0.038
300.1	0.69 ± 0.04	0.318 ± 0.031
305.0	0.70 ± 0.02	0.332 ± 0.030
307.4	0.62 ± 0.02	0.504 ± 0.019
309.9	0.67 ± 0.05	0.553 ± 0.016
312.4	0.66 ± 0.03	0.609 ± 0.017

The values of A_μ and A_p depend on the angle between the rotation axis of the molecule and the applied magnetic field, θ

$$A_X = A_X^{iso} + \frac{1}{2}D_X^{\parallel}(3\cos^2\theta - 1) \tag{7}$$

In the case of a macroscopically aligned liquid crystal with $\hat{n}$ oriented along the magnetic field, the orientationally averaged hfccs, $\langle A_X\rangle$, are given by

$$\langle A_X\rangle = A_X^{iso} + \langle D_X^{\parallel}\rangle S \tag{8}$$

where $\langle D_X^{\parallel}\rangle$ is the motionally averaged muon dipolar hfcc. $\langle D_\mu^{\parallel}\rangle$ has been calculated using eq 2 (assuming that $T_{N-I} = 314$ K) and eq 8. $\langle D_p^{\parallel}\rangle$ decreases approximately linearly with increasing temperature in the N phase due to the fluctuations of the radical about its average orientation. We have assumed a simple "wobbling in a cone" model where there is equal probability for $0 < \phi < \phi_c$ and $\pi - \phi_c < \phi < \pi$ and zero probability for $\phi_c < \phi < \pi - \phi_c$ (ϕ is the angle between the instantaneous long axis of the radical and the cone axis). Israelachvili et al. have derived expressions for the hyperfine parameters of a spin probe rotating rapidly about the long molecular axes and simultaneously wobbling within a cone.[40] It can be shown that this motion leads to

$$\langle D_X^{\parallel}\rangle = D_X^{\parallel}\left(\frac{\cos\phi_c + \cos^2\phi_c}{2}\right) \tag{9}$$

The value of $D_p^{\parallel}$, i.e., for pure uniaxial rotation, can be estimated by extrapolating to the temperature where the sample crystallized, which we found to be ~280 K, and this has a value of 0.824 MHz. The values of ϕ_c as a function of temperature are listed in Table 3. It is the estimation of $D_p^{\parallel}$ that introduces the largest systematic error in determining the amplitude of the fluctuations. The mean-squared fluctuation amplitude, $\langle\phi^2\rangle$, has been calculated from ϕ_c and increases approximately linearly in the N phase 6, although the fluctuations are much smaller than in the cyanobiphenyl LC, where $\phi_c \rightarrow \pi/2$ as $T \rightarrow T_{N-I}$. de Gennes and Prost estimated that for a rod-like molecule $\langle\phi^2\rangle$ is given by

$$\langle\phi^2\rangle \approx \frac{k_B T q_c}{\pi^2 K} \tag{10}$$

where k_B is the Boltzmann constant, T is the temperature, q_c is an upper cutoff wave vector, and K is the average Frank elasticity constant.[1] Our results are consistent with the preceding equation only if the intermolecular interaction energy ($\sim K/q_c$) is temperature independent. K itself depends strongly on temperature,[41] with de Gennes and Prost noting that $K \sim S^2$.[1] The smaller amplitude

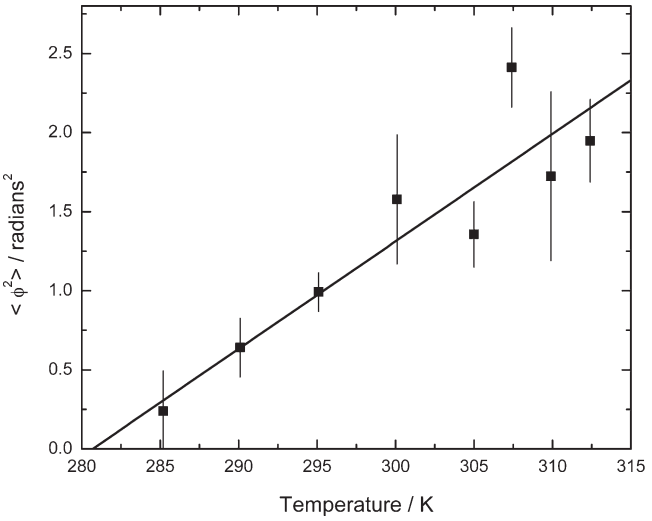

Figure 6. Temperature dependence of the mean-squared fluctuation amplitude of MBBA about the local director in the nematic phase.

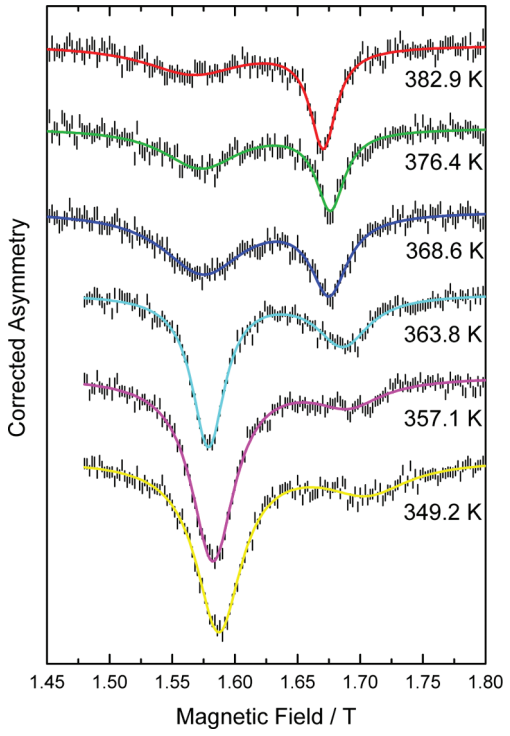

Figure 7. ALC-μSR spectra of CN in the isotropic and chiral nematic phases. The I−N* phase transition occurs at 364.3 K. The solid lines are the best fits to the experimental data.

fluctuations in MBBA compared with 5CB and 8CB suggests that the intermolecular interaction energy of MBBA is larger than that of the cyanobiphenyl LC.

Cholesteryl Nonanoate. Representative ALC-μSR spectra of CN in the N* and I phases are shown in Figure 7. There are two Lorentzian-shaped resonances between 1.5 and 1.8 T. The lower field resonance narrows with increasing temperature in the N* and then broadens and decreases in amplitude with increasing temperature in the I phase. This resonance was not observed above 383 K as it had broadened to such an extent that it could not be distinguished from the background. The higher field resonance narrows with increasing temperature in both the N* and I phases.

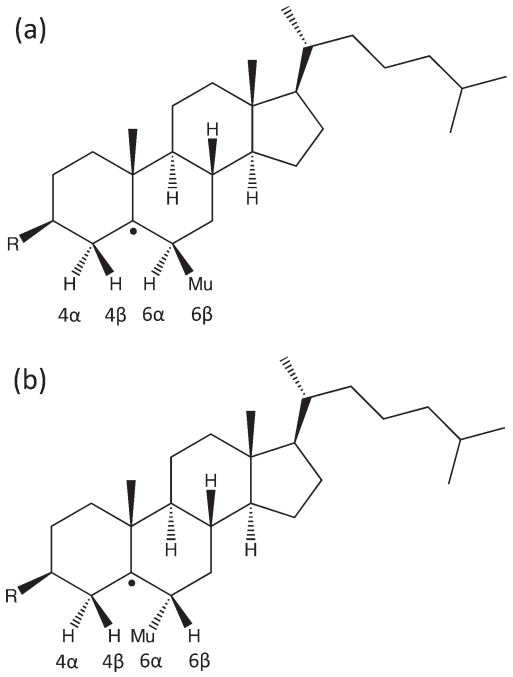

Figure 8. Structures of the Mu adducts of cholesteryl nonanoate: (a) Mu-6β-CN and (b) Mu-6α-CN. R = O—C(=O)—C_8H_{17}.

Table 4. Calculated (UB3LYP/6-31G(d,p)//UPBE0/EPR-II) Muon and Proton Hyperfine Coupling Constants ($|A_p|$ > 10 MHz) and the Corresponding ALC Resonance Fields for the Mu Adducts of CN

radical	nucleus	A_X/MHz	B_{res}/T
Mu-6α-CN	$H_{4\alpha}$	20.53	0.2733
	$H_{4\beta}$	120.41	0.2588
	$Mu_{6\alpha}$	71.65[a]	0.2630
	$H_{6\beta}$	108.76[b]	0.1964
Mu-6β-CN	$H_{4\alpha}$	20.53	2.2582
	$H_{4\beta}$	120.41	1.7192
	$H_{6\alpha}$	17.63[b]	2.2738
	$Mu_{6\beta}$	441.92[a]	1.6223

[a] A_μ calculated by multiplying DFT value by 3.183 to account for γ_μ/γ_p and by 1.20 to account for the primary isotope effect. [b] A_p calculated by multiplying DFT value by 0.94 to account for the secondary isotope effect.

Paramagnetic spin probes can be produced by the addition of Mu to the C=C bond of CN. Two types of radicals can be formed, which differ in the spatial arrangement of the muon (Figure 8). The radicals will be referred to in terms of the position of Mu with the Mu-6β-CN radical having Mu is in the 6β position, while Mu-6α-CN in the 6α position. Mu addition is not observed at a tertiary carbon when secondary carbons are present.[42] The calculated hfccs and resonance fields for Mu-6α-CN and Mu-6β-CN are listed in Table 4 and on the basis of the good agreement between the calculated and experimental values we can conclude that the lower-field resonance is the Δ_1 resonance of radical Mu-6β-CN and the higher-field resonance

dx.doi.org/10.1021/jp203006w |J. Phys. Chem. B 2011, 115, 9360–9368

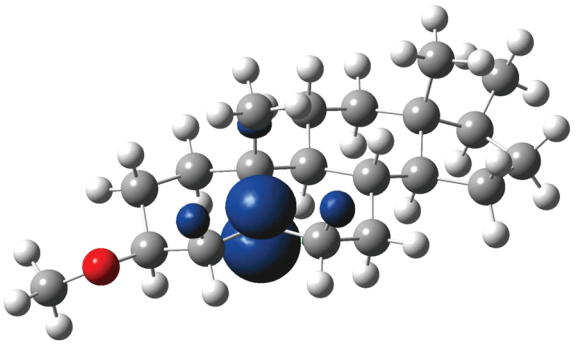

Figure 9. Unpaired electron spin density distribution in H adduct of cholesteryl nonanoate. UB3LYP/6-31G(d,p)//UPBE0/EPR-II with isospin density =0.004. There is significant spin density at positions 4β and 6β.

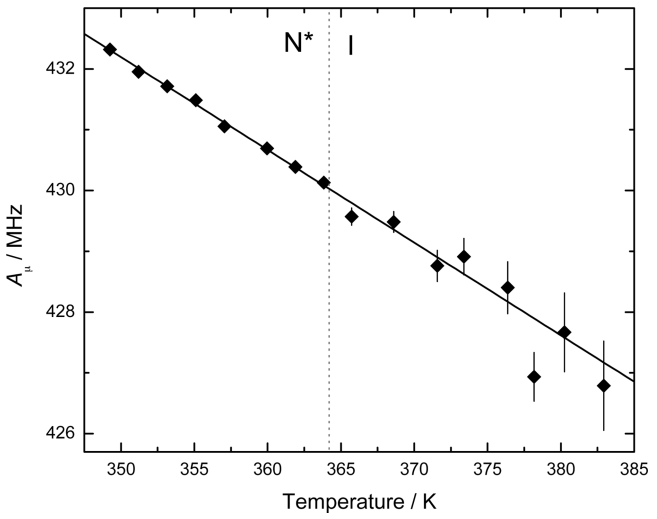

Figure 10. Temperature dependence of the muon hyperfine coupling constant of Mu-6β-CN. The solid line is the best fit to the experimental data. The dotted line denotes the N*−I phase transition.

is the Δ_0 resonance of $H_{4\beta}$ of radical Mu-6β-CN. Resonances due to radical Mu-6α-CN were not observed because of the very small muon hfcc that results from the C-Mu bond lying almost in the nodal plane of the SOMO (Figure 9). The calculated principal components of the muon hyperfine tensor of Mu-6β-CN are −16.56, −11.88, and +28.44 MHz, so the static hyperfine tensor is approximately axially symmetric.

A_μ decreased linearly with increasing temperature and there was no shift at the phase transition, as has been observed for MBBA and the cyanobiphenyl LC, due to CN not being macroscopically aligned (Figure 10) . The decrease of A_μ ($dA_\mu/dT = -0.160 \pm 0.007$ MHz K^{-1}) is due to increased torsional motion of the steroidal ring system that decreases the overlap between the muon and the SOMO. The Δ_1 resonance width and amplitude change significantly with temperature. The width decreased in the N* phase and was at a minimum at T_{N^*-I}, then increased dramatically in the I phase (Figure 11). The change in the Δ_1 resonance width and amplitude is due to the motion of the radical. The narrowness of the Δ_1 resonance in the N* phase compared with the values of the static hyperfine tensor suggests that the radical is undergoing rapid uniaxial rotation.

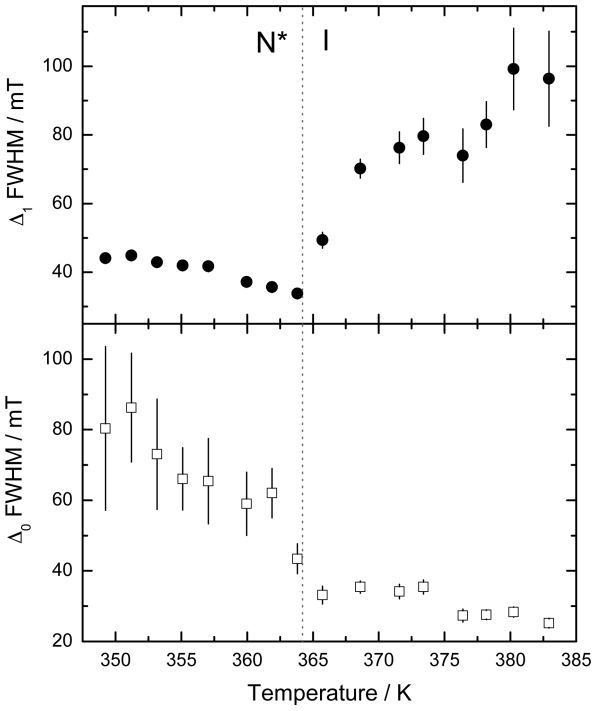

Figure 11. Temperature dependence of the fwhm of the Δ_1 and Δ_0 resonances of Mu-6β-CN. The dotted line denotes the N*−I phase transition.

Table 5. Temperature Dependence of the Muon Dipolar hfcc of Mu-6β-CN and Maximum Fluctuation Angle, ϕ_c, in the N* Phase of CN

T/K	$\lvert\langle D_\mu^\parallel\rangle\rvert$/MHz	ϕ_c/radians
349.2	3.98 ± 0.13	0.24 ± 0.13
351.2	4.05 ± 0.10	0.10 ± 0.10
353.2	3.88 ± 0.12	0.45 ± 0.13
355.1	3.79 ± 0.11	0.64 ± 0.13
357.1	3.77 ± 0.12	0.70 ± 0.13
360.0	3.36 ± 0.10	1.66 ± 0.13
361.9	3.22 ± 0.09	2.02 ± 0.11
363.8	3.05 ± 0.10	2.47 ± 0.14

In the N* phase the rapidly rotating radical wobbles about the local director and as the temperature increases the amplitude of the motion increases and this leads to a decrease in the dipolar muon hfcc. A similar trend was observed for the Δ_1 resonance of one of the Mu adducts of C_{70}.[43] The magnitude of $\langle D_\mu^\parallel\rangle$ was determined from the width of the Δ_1 resonance ($\lvert\langle D_\mu^\parallel\rangle\rvert$ = 2/3 fwhm γ_μ) and the values as a function of temperature are reported in Table 5. As noted in the previous section the motionally averaged muon dipolar hfcc, $\langle D_\mu^\parallel\rangle$, is related to the fluctuation amplitude about the local director by eq 9. We attempted to calculate $D_\mu^\parallel$ using the hyperfine tensor obtained from the DFT calculations and assuming the rotation axis to coincide with minor principal axis of the moment of inertia but it was found that a small change in the orientation axis has a large effect on $D_\mu^\parallel$, so this approach was abandoned. We note that $\lvert\langle D_\mu^\parallel\rangle\rvert$ approaches a value of ~4.1 MHz as the sample was cooled to the SmA−N* phase transition and we made the assumption at

dx.doi.org/10.1021/jp203006w |J. Phys. Chem. B 2011, 115, 9360–9368

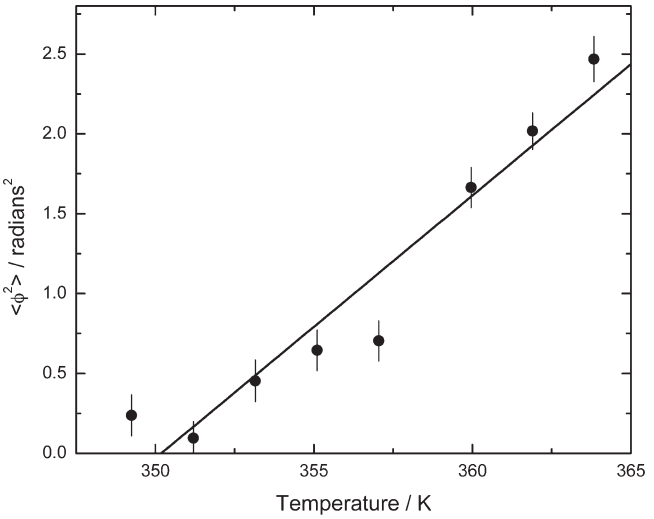

Figure 12. Temperature dependence of the mean-squared fluctuation amplitude about the local director in the N* phase.

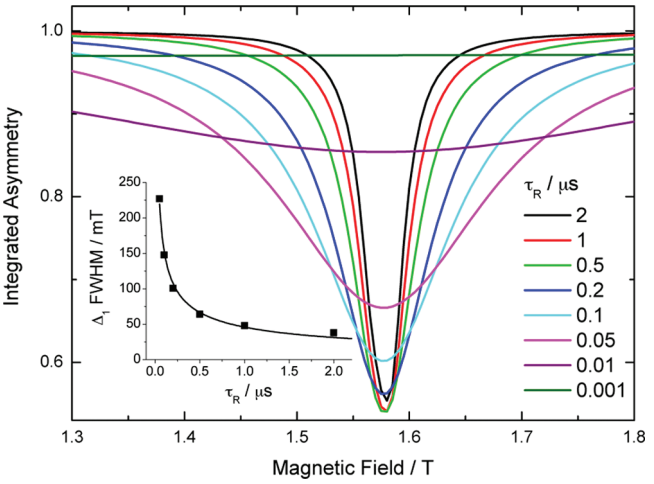

Figure 13. Simulated Δ_1 resonance for a radical undergoing pseudo isotropic reorientation with A_μ = 430 MHz and $D_\mu^{\parallel}$ = −4.1 MHz as a function or rotational correlation time, τ_R. The inset graph shows the dependence of the Δ_1 resonance fwhm on τ_R. The simulations were performed with the Quantum spin simulation program.[45]

that point that $\phi_c \rightarrow 0$ and $D_\mu^{\parallel}$ = −4.1 MHz. The values of ϕ_c as a function of temperature were determine using eq 9 and are reported in Table 5. $\langle\phi^2\rangle$ increases approximately linearly with temperature in the N* phase and the fluctuation amplitude about $\hat{n}$ is similar to that of MBBA but less than in 5CB and 8CB (Figure 12).

The Δ_1 resonance in the I phase broadens and decreases in amplitude due to slow isotropic reorientation. Similar behavior was observed for the Mu adduct of C_{60}.[44] The effects of slow isotropic reorientation on the ALC-μSR spectra were simulated using the Quantum spin simulation program (Figure 13).[45] The muon hfcc used for the simulations was 430 MHz and we have assumed an axial dipolar tensor resulting from fast uniaxial rotation with $D_\mu^{\parallel}$ = −4.1 MHz. In the simulations we introduced 20 evenly distributed orientations (given by the vertices of a dodecahedron) and allowed the radical to hop to adjacent orientations. The simulated resonances are qualitatively consistent with

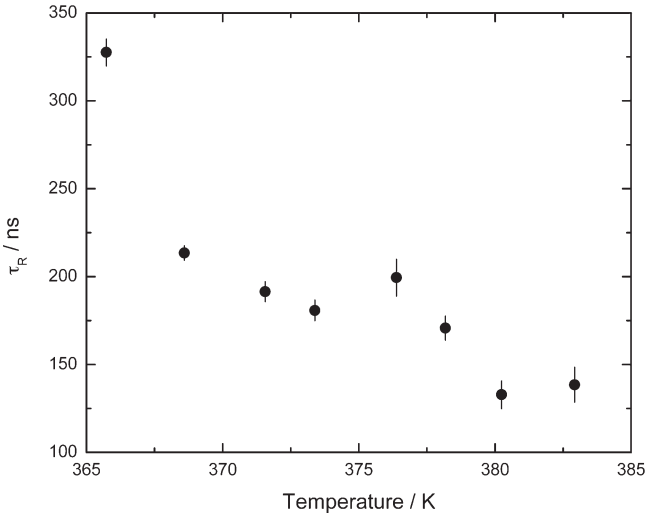

Figure 14. Temperature dependence of the rotational diffusion time of CN in the isotropic phase.

those reported by Tregenna-Piggott et al.[46] The results of the simulations made it possible to determine the relationship between the rotational correlation time (τ_R) and the Δ_1 line width and hence to determine τ_R of CN in the I phase (Figure 14). The value of τ_R decreases from 328 ± 8 ns just above T_{N^*-I} to 138 ± 10 ns at 383 K. The decrease of τ_R is roughly proportional to T^{-1} but there is considerable scatter.

CONCLUSIONS

Paramagnetic muoniated spin probes were produced by Mu addition to MBBA and CN and observed with ALC-μSR spectroscopy. The hfccs of the Mu-C_8-MBBA radical shift in the N phase due to the ordering of the molecules along the magnetic field and the dipolar coupling, which is modulated by fluctuations of the radical about the local director. The extent of these fluctuations was determined from the temperature dependence of the methylene proton hfcc and the mean-squared fluctuation amplitude increased linearly with temperature. The temperature dependence of the Δ_1 resonance line width of the Mu-6β-CN radical has been employed to probe the motion of the molecules. In the N* phase the sample consists of many domains and the molecules fluctuate about a mean orientation with a mean-squared fluctuation amplitude that increases linearly with temperature while in the I phase the molecules undergo slow isotropic reorientation.

ASSOCIATED CONTENT

Supporting Information. The optimized structures of all molecules described in this paper. This material is available free of charge via the Internet at http://pubs.acs.org.

AUTHOR INFORMATION

Corresponding Author

*E-mail: iain.mckenzie@triumf.ca. Phone: 1 604 222 7386. Fax: 1 604 222 1074.

Present Addresses

§Centre for Molecular and Materials Science, TRIUMF, Vancouver, B.C. Canada.

■ ACKNOWLEDGMENT

Support from the staff at the Laboratory for Muon Spin Spectroscopy at the Paul Scherrer Institute is gratefully acknowledged. This research project has been supported by the European Commission under the seventh Framework Programme through the "Research Infrastructures" action of the "Capacities Programme", Contract No. CP-CSA_INFRA-2008-1.1.1 Number 226507-NMI3. Computing resources provided by STFC's e-Science facility. Dr. J. S. Lord is thanked for assistance with the Quantum spin simulation program.

■ REFERENCES

(1) de Gennes, P. G.; Prost, J. *The Physics of Liquid Crystals*, 2nd ed.; Oxford University Press: New York, 1993.
(2) Collings, P. J.; Hird, M. *Introduction to Liquid Crystals: Chemistry and Physics*; Taylor and Francis Ltd.: London, 1997.
(3) Chandrasekhar, S. *Liquid Crystals*, 2nd ed.; Cambridge University Press: New York, 1992.
(4) Kneppe, H.; Reiffenrath, V.; Schneider, F. *Chem. Phys. Lett.* **1982**, *87*, 59–62.
(5) McMillan, W. L. *Phys. Rev. A* **1972**, *6*, 936–947.
(6) Dong, R. Y. *Nuclear Magnetic Resonance of Liquid Crystals*, 2nd ed.; Springer-Verlag: New York, 1997.
(7) Burnell, E. E.; de Lange, C. A. *Chem. Rev.* **1998**, *98*, 2359–2387.
(8) Pines, A.; Chang, J. J. *Phys. Rev. A* **1974**, *10*, 946–949.
(9) Dong, R. Y.; Shen, X. *J. Phys. Chem. A* **1997**, *101*, 4673–4678.
(10) Polnaszek, C. F.; Freed, J. H. *J. Phys. Chem.* **1975**, *79*, 2283–2306.
(11) Casini, R.; Faetti, S.; Martinelli, M.; Santucci, S.; Giordano, M. *J. Magn. Reson.* **1977**, *26*, 201–207.
(12) Spielberg, J. I.; Gelerinter, E. *Chem. Phys. Lett.* **1982**, *92*, 184–186.
(13) Atherton, N. M.; Shohoji, M. C. B. *J. Chem. Soc. Faraday Trans. 2* **1983**, *79*, 1243–1247.
(14) Luz, Z.; Poupko, R.; Samulski, E. T. *J. Chem. Phys.* **1981**, *74*, 5825–5837.
(15) McKenzie, I.; Roduner, E. *Naturwissenschaften* **2009**, *96*, 873–887.
(16) Kochi, J. K. In *Advances in Free-Radical Chemistry*; Williams, G. H., Ed.; Academic Press: New York, 1975; Vol. 5, Chapter 4.
(17) Roduner, E. *The Positive Muon as a Probe in Free Radical Chemistry - Potential and Limitations of the μSR Techniques (Lecture Notes in Chemistry)*; Springer: Berlin, 1988; Vol. 49.
(18) Roduner, E. *Chem. Soc. Rev.* **1993**, *22*.
(19) Blundell, S. J. *Chem. Rev.* **2004**, *104*, 5717–5735.
(20) Yaouanc, A.; de Réotier, P. D. *Muon Spin Rotation, Relaxation, and Resonance, Applications to Condensed Matter*; Oxford University Press: New York, 2010.
(21) Scheuermann, R.; Tucker, I. M.; Creeth, A. M.; Dilger, H.; Beck, B.; Roduner, E. *Phys. Chem. Chem. Phys.* **2002**, *4*, 1510–1512.
(22) Scheuermann, R.; Tucker, I. M.; Dilger, H.; Staples, E. J.; Ford, G.; Fraser, S. B.; Beck, B.; Roduner, E. *Langmuir* **2004**, *20*, 2652–2659.
(23) Martyniak, A.; Dilger, H.; Scheuermann, R.; Tucker, I. M.; McKenzie, I.; Vujosevic, D.; Roduner, E. *Phys. Chem. Chem. Phys.* **2006**, *8*, 4723–4740.
(24) Martyniak, A.; Dilger, H.; McKenzie, I.; Scheuermann, R.; Lagerwall, J.; Roduner, E. *Colloids Surf., A* **2007**, *309*, 224–230.
(25) Dawin, U.; Dilger, H.; Roduner, E.; Scheuermann, R.; Stoykov, A.; Giesselmann, F. *Angew. Chem., Int. Ed.* **2009**, *49*, 2427–2430.
(26) Lovett, B. W.; Stiessberger, J.; Blundell, S. J.; Jestädt, T.; Ardavan, A.; Marshall, I. M.; Pratt, F. L.; Reid, I. D. *Physica B* **2000**, *289−290*, 612–615.
(27) Lovett, B. W.; Blundell, S. J.; Stiessberger, J. S.; Pratt, F. L.; Jestädt, T.; Hayes, W.; Reid, I. D. *Phys. Rev. B* **2001**, *63*, 054204.
(28) McKenzie, I.; Dilger, H.; Stoykov, A.; Scheuermann, R. *J. Phys. Chem. B* **2009**, *113*, 10135–10142.
(29) McKenzie, I.; Dilger, H.; Scheuermann, R.; Stoykov, A. *J. Phys.: Conf. Ser.* **2010**, *225*, 012034.
(30) McKenzie, I.; Cammidge, A. N.; Dilger, H.; Gopee, H.; Scheuermann, R.; Stoykov, A.; Jayasooriya, U. A. *Phys. Chem. Chem. Phys.* **2010**, *12*, 9900–9908.
(31) Dilger, H.; Martyniak, A.; Scheuermann, R.; Vujosevic, D.; Tucker, I. M.; McKenzie, I.; Roduner, E. *Physica B* **2006**, *374−375*, 317–320.
(32) http://lmu.web.psi.ch/facilities/alc/alc.html.
(33) http://root.cern.ch.
(34) Frisch, M. J. et al. *Gaussian 03*, revision B.05; Gaussian, Inc.: Pittsburgh, PA, 2003.
(35) Improta, R.; Barone, V. *Chem. Rev.* **2004**, *104*, 1231–1253.
(36) Brodovitch, J.-C.; Addison-Jones, B.; Ghandi, K.; McKenzie, I.; Percival, P. W.; Schüth, J. *Can. J. Chem.* **2003**, *81*, 1–6.
(37) Rhodes, C. J.; Morris, H.; Reid, I. D. *Magn. Reson. Chem.* **2001**, *39*, 438–442.
(38) Hoshino, T.; Kubo, A.; Imashiro, F.; Terao, T. *Mol. Phys.* **1998**, *93*, 301–313.
(39) Yu, D.; Percival, P. W.; Brodovitch, J.-C.; Leung, S.-K.; Kiefl, R. F.; Venkateswaran, K.; Cox, S. F. *J. Chem. Phys.* **1990**, *142*, 229–236.
(40) Israelachvili, J.; Sjösten, J.; Eriksson, L. E. G.; Ehrström, M.; Gräslund, A.; Ehrenberg, A. *Biochim. Biophys. Acta* **1975**, *382*, 125–141.
(41) Haller, I. *J. Chem. Phys.* **1972**, *57*, 1400–1405.
(42) Brodovitch, J.-C.; Ghandi, K.; McKenzie, I.; Percival, P. W.; Schüth, J. *Physica B* **2006**, *374−375*, 310–313.
(43) Dennis, T. J. S.; Prassides, K.; Roduner, E.; Cristofolini, L.; DeRenzi, R. *J. Phys. Chem.* **1993**, *97*, 8553–8556.
(44) Roduner, E.; Prassides, K.; Macrae, R. M.; Thomas, I. M.; Niedermayer, C.; Binninger, U.; Bernhard, C.; Hofer, A.; Reid, I. D. *Chem. Phys.* **1995**, *192*, 231–237.
(45) Lord, J. S. *Physica B* **2006**, *374−375*, 472–474.
(46) Tregenna-Piggott, P. L. W.; Roduner, E.; Santos, S. *Chem. Phys.* **1996**, *203*, 317–337.